Development of Holographic Techniques to Study Thermally Induced Deformation

Holographic methods are developed which accurately determine deformation in thermally anisotropic materials

by J.A. Gilbert and D.T. Vedder

ABSTRACT—Holography is used to study thermally induced deformation in a rock specimen extracted from a cubical sample taken during a geological survey. Experiments are conducted over small temperature increments, on the order of a few degrees Fahrenheit, to suppress extraneous variations in optical path which could otherwise be introduced by temperature gradients and convection currents in the air surrounding the specimen. The concept of an optical rosette is introduced to predict principal strains and their corresponding directions from holographically obtained data. Values measured for thermal coefficients of expansion fall within the range of those documented by other investigators using more conventional experimental methods.

List of Symbols

$\mathbf{d}$ = displacement vector
$\mathbf{e}_i, \mathbf{e}_i'$ = propagation vector
$\hat{\mathbf{e}}_i, \hat{\mathbf{e}}_i'$ = unit vector in direction of propagation
$\mathbf{i}_i$ = unit vector along cartesian axis
n_m = moiré-fringe order number
$\mathbf{n}_s$ = surface normal
u_i = scalar component of displacement
v_i = principal direction
P = point in space
T, T_i = temperature
X_i, X_i' = cartesian coordinate axes
α = thermal coefficient of expansion
α_i = thermal coefficient of expansion along principal-strain direction
β = sensitivity angle
γ = angle of bodily rotation
δ_{ij} = Kronecker Delta
ϵ_{ij} = strain-tensor component
$\epsilon_A, \epsilon_B, \epsilon_C$ = experimentally measured normal strain
λ = wavelength
λ_{ij} = direction cosine
ϕ_i = principal thermal strain
ϕ_{ij}, ϕ_{ij}' = thermal strain
ϕ_A, ϕ_B, ϕ_C = experimentally determined thermal strain
Δ = change in
θ = angle of orientation
θ_i = angle of orientation for principal strain
Λ = transformation tensor
Φ, Φ' = thermal-strain tensor

J.A. Gilbert (SESA Member) is Assistant Professor of Engineering Mechanics, University of Wisconsin-Milwaukee, Milwaukee, WI 53201. D.T. Vedder is presently associated with National Water Lift Co., Kalamazoo, MI 49001.

Paper was presented at 1979 SESA Spring Meeting held in San Francisco, CA on May 20-25.

Original manuscript submitted: July 6, 1979. Final version received: May 23, 1980.

Introduction

Underground space is a new resource which provides urban areas or their proximity with a complete subsurface layer of services, including both storage and activity functions. An important aspect of underground-space utilization is the analysis of temperature-induced stress, strain and displacement encountered in the neighborhood of tunnels used for hot or cold storage. Experience gained in the storage of oil shows that rock usually offers cheap storage with small heat losses[1]; however, rock caverns which contain fuel oil, steam, hot water or nuclear waste are subjected to a thermal-stress field,[2-4] in addition to in-situ and excavation stresses. This paper establishes a holographic method which can ultimately be used to predict thermal behavior of core samples taken during a geological survey. Moreover, the method of attack outlined in this investigation is applicable to any thermally anisotropic material, particularly for those which have positive thermal coefficients of expansion.

Holography can be used to determine thermally induced deformation; however, it is advisable to conduct experiments over small temperature increments on the order of a few degrees Fahrenheit, to suppress extraneous variations in optical path which could otherwise be introduced by temperature gradients and convection currents in the air surrounding the specimen.

The strain on a two-dimensional surface can be measured if two full-field displacement patterns are recorded, each of which corresponds to a different displacement component. Two direct and two cross derivatives must be evaluated at each point. In this investigation, strain is homogeneous; however, the holographic-fringe patterns have relatively few fringes since the thermal coefficients of expansion of rock are small. This makes it difficult to evaluate derivatives corresponding to shear, especially close to the principal directions of strain, along which these quantities vanish. We introduce the concept of the optical rosette to facilitate the analysis of thermally induced deformation. This technique requires the evaluation of direct derivatives but does not require the evaluation of cross derivatives. The direct derivative never vanishes for a material whose thermal coefficients of expansion are

positive. Although three displacement patterns are necessary to completely evaluate thermal properties in the two-dimensional case, only three derivatives, as opposed to four, are required in this method.

A rock specimen which is considered homogeneous is subjected to a uniform temperature rise. Full-field displacement patterns are obtained using a holographic-moiré technique. These patterns are analyzed for strain due to the increase in temperature; and, transformation equations are applied to predict principal strains and their corresponding directions. Values obtained for thermal coefficients of expansion fall within the range of those documented by other investigators using more conventional experimental methods.

This study establishes holography as a useful tool in rock mechanics and opens the door to coupled analytical and experimental investigations in the area. Specific contributions made by the authors include adopting holography to measure thermally induced strain in rock, developing an experimental setup which uses a low-powered laser and introducing the optical-rosette concept.

Statement of the Problem—Analysis

A specimen was cut from a one foot (30.5 cm) cubical block of Bedford limestone collected from a quarry as one of many samples taken from a geological survey carried out by the United States Bureau of Mines (USBM) and the Advanced Research Projects Agency (ARPA). These samples were distributed to investigators throughout the United States for application and study in the field of rock mechanics. A right, rectangular prismatic specimen which measured 2.5 × 2.5 × 0.5 in. (6.34 × 6.35 × 1.27 cm) was cut from the cube provided for analysis. The cartesian-axes system shown in Fig. 1 was assigned to the specimen for reference purposes.

Bedford limestone is sedimentary in nature and usually forms in parallel layers or strata. It was evident from visual inspection along each edge of the specimen that stratification was parallel to the X_3 axis. These sedimentary layers, oriented perpendicular to the X_1X_2 plane, are pictorially represented in Fig. 1. We assume that the principal thermal coefficients of expansion are directly dependent on stratification; that they are independent of direction in planes parallel to rock layers but take on a different value normal to them. Consequently, the thermal coefficients of expansion will be directionally dependent in the X_1X_2 plane and a uniform temperature change will not produce equal expansions in all directions.

It is convenient to define a thermal-strain tensor, Φ, such that

$$\Phi_{ij} = \frac{\epsilon_{ij}}{\Delta T} \tag{1}$$

where ΔT is the uniform temperature increment initiated to the specimen to cause strains ϵ_{ij}; and, by definition, the principal values of Φ are the principal thermal coefficients of expansion.

Thermally induced surface strain which results from the overall thermal behavior of the rock sample can now be formulated as a tensor quantity which is governed by the transformation

$$\Phi_{ij}' = \lambda_{ik}\lambda_{jl}\Phi_{kl} \tag{2}$$

where Φ_{ij}', Φ_{ij} and λ_{ij} are respectively the components of the transformed tensor, Φ', the original tensor, Φ; and, the matrix, Λ, whose components denote the cosine of the angle between the i^{th} primed and j^{th} unprimed coordinate axes.

Equation (2) transforms a tensor initially specified in the reference-axes system to a primed system. Once a tensor, Φ, has been established, it is possible to transform to primed axes which correspond to the principal directions, or, eigenvectors, associated with the principal values, or eigenvalues, of Φ, by solving,

$$(\phi_{ij} - \delta_{ij}\alpha)\nu_j = 0 \tag{3}$$

where δ_{ij} is the Kronecker Delta and α are the principal values; or, thermal coefficients of expansion measured along the corresponding principal directions of Φ given by ν_j.

It was previously ascertained that layers in the specimen were oriented perpendicular to the X_1X_2 plane. Consequently, the lateral surface of the rock specimen under investigation lies in a principal plane. Under this assumption, the thermal-strain tensor referred to the reference axes system shown in Fig. 1 takes the form

$$\Phi = [\Phi_{ij}] = \begin{bmatrix} \phi_{11} & \phi_{12} & 0 \\ \phi_{21} & \phi_{22} & 0 \\ 0 & 0 & \phi_{33} \end{bmatrix} \tag{4}$$

Two-dimensional transformation laws can be used to determine the eigenvalues, ϕ_1 and ϕ_2, and their corresponding eigenvectors for the two-dimensional situation in

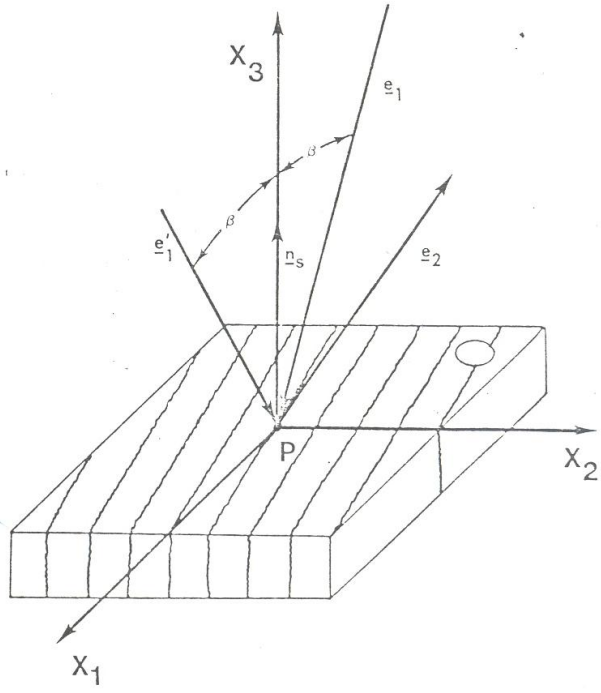

Fig. 1—Model and illumination—Pictorial representation of sedimentary layers

the X_1X_2 plane. The third eigenvalue ϕ_{33}, defined as ϕ_3, will be the same as the principal thermal coefficient of expansion measured parallel to the rock layers in the X_1X_2 plane.

In general, these tensor transformations are valid on a pointwise basis. In this investigation, however, the model is assumed to be homogeneous and is subjected to a uniform temperature change. The corresponding strain field is also homogeneous and the same transformation can be applied to all points in the X_1X_2 plane.

Holographic measurements must be made so that transformation equations can be applied to predict principal thermal coefficients of expansion and their corresponding directions.

Holographic-displacement Analysis—The Optical Rosette

The holographic-moiré technique[6,7] is applied to the flat surface of the rock specimen in the X_1X_2 plane. As shown in Fig. 1, two equally intense object beams, $\mathbf{e}_1$ and $\mathbf{e}'_1$, are contained in the X_1X_3 plane and illuminate a point P on the X_1X_2 plane of the rock surface. These illuminations make equal angles with respect to the surface normal, $\mathbf{n}_3$. Laser light is diffused off the model surface, from point P, to the hologram along propagation vector $\mathbf{e}_2$. When the double-exposure method is used to determine thermally induced deformation, two double-exposure holograms are recorded; one due to each object beam. During reconstruction, these component patterns optically superimpose and a moiré pattern is formed which is characterized by

$$\lambda n_m = (\hat{\mathbf{e}}_1 - \hat{\mathbf{e}}_1') \cdot \mathbf{d} \tag{5}$$

where λ is the wavelength, n_m is the moiré-fringe order number, $\mathbf{d}$ is the displacement vector and $\hat{\mathbf{e}}_1$, $\hat{\mathbf{e}}_1'$ are unit vectors in the direction of propagation. $\hat{\mathbf{e}}_1$ and $\hat{\mathbf{e}}_1'$ can be expressed in terms of the reference-axes system as

$$\hat{\mathbf{e}}_1' = -\sin\beta\,\mathbf{i}_1 - \cos\beta\,\mathbf{i}_3 \tag{6}$$

and

$$\hat{\mathbf{e}}_1 = \sin\beta\,\mathbf{i}_1 - \cos\beta\,\mathbf{i}_3 \tag{7}$$

where $\mathbf{i}_1$, $\mathbf{i}_2$, $\mathbf{i}_3$ are unit vectors along X_1, X_2, X_3, respectively, and β is the sensitivity angle. Substituting eqs (6) and (7) into eq (5),

$$\lambda n_m = (2\sin\beta\,\mathbf{i}_1) \cdot (u_1\mathbf{i}_1 + u_2\mathbf{i}_2 + u_3\mathbf{i}_3) \tag{8}$$

where u_1, u_2, u_3 are the scalar displacement projections along X_1, X_2, X_3, respectively. Performing the dot product and solving,

$$u_1 = \frac{\lambda n_m}{2\sin\beta} \tag{9}$$

The moiré evident through optical superposition of the two component patterns, gives the projection of the displacement of point P in a sensitivity direction which coincides with the X_1 axis for the position of the model shown in Fig. 1. Equation (9) was derived for point P; however, if $\mathbf{e}_1$ and $\mathbf{e}_1'$ are the same for all model points, this equation is valid on a full-field basis. The latter can be physically accomplished by collimating each illumination.

There are several significant features of the holographic-moiré method; namely,

(1) There is no sensitivity to the other in-plane displacement component u_2; or, to the out-of-plane component, u_3.

(2) The viewing direction, corresponding to $\mathbf{e}_2$, is usually chosen normal to the surface; however, no error is introduced if this is not the case.

(3) The sensitivity angle β can be adjusted to measure displacement with sensitivity throughout the entire holographic range.

The thermal-strain tensor is completely defined for all points in the X_1X_2 plane if one measures u_1 and u_2 over the full field. That is,

$$\phi_{11} = \frac{1}{\Delta T}\left(\frac{\partial u_1}{\partial X_1}\right)$$

$$\phi_{22} = \frac{1}{\Delta T}\left(\frac{\partial u_2}{\partial X_2}\right) \tag{10}$$

$$\phi_{12} = \phi_{21} = \frac{1}{\Delta T}\left(\frac{\partial u_1}{\partial X_2} - \frac{\partial u_2}{\partial X_1}\right)$$

These derivatives can be determined graphically; or, optically with the methods described in Refs. 8 and 9.

Certain rigid-body movements of the object produce fringe effects. When the surface lies in the X_1X_2 plane and is illuminated with beams contained in the X_1X_3 plane, the most significant of these is rotation about the X_3 axis. This produces straight, uniformly spaced fringes parallel to the X_1 axis, thereby causing confusion with fringes representing shear. This effect is eliminated when two sets of illuminations are used, one in the X_1X_3 plane and the other in the X_2X_3 plane.[10] That is, the interferogram from the X_1X_3 plane beams provides ϕ_{11} and an apparent shear component composed of $\frac{1}{\Delta T}\frac{\partial u_1}{\partial X_2}$ plus $\frac{\gamma}{\Delta T}$, where γ is the unknown angle of bodily in-plane rotation (if one occurs). Likewise the X_2X_3 plane beams provide ϕ_{22} and the apparent shear composed of $\frac{1}{\Delta T}\frac{\partial u_2}{\partial X_1}$ plus $\frac{\gamma}{\Delta T}$. Subtraction of the two shear components gives,

$$\phi_{12} = \phi_{21} = \frac{1}{\Delta T}\left(\frac{\partial u_1}{\partial X_2} - \frac{\partial u_2}{\partial X_1}\right) \tag{11}$$

which is independent of γ.

A rotation of the surface about the X_3 axis causes uniform fringes with a spacing in the X_1 direction but with far less sensitivity than that caused by the in-plane rotation already mentioned.

A single interferogram alone does not reveal whether the thermal strain is tensile or compressive, nor the sense of the shear strain; however, the fact that most materials, including rock, have positive thermal coefficients of expansion allows us to deduce this information.

In this investigation, the cross derivatives were not easy to evaluate. The accuracy in measuring these quantities improves as the density of the holographic-moiré-fringe pattern increases. Unfortunately, one of the major problems associated with the holographic determination of displacement arising from thermal causes is that extraneous variations may occur in the optical path which are introduced by temperature gradients and convection currents in the surrounding air. These effects can be suppressed by testing over a small temperature range, preferably close to room temperature. When the thermal

coefficients of expansion of the specimen are small, the holographic-moiré pattern does not contain a great many fringes and it is virtually impossible to evaluate the cross derivatives along a sensitivity direction close to an eigenvector of the thermal-strain tensor since these quantities are identically zero along the principal directions.

We now introduce the concept of an optical rosette to eliminate this problem, capitalizing on the fact that most materials, including rock, have thermal coefficients of expansion which are positive. Consequently, the direct derivative of the holographic-moiré pattern along the sensitivity direction is never zero for any orientation of the specimen. Furthermore, when the model lies in the X_1X_2 plane and is illuminated with beams contained in the X_1X_3 plane, rotation about X_3 does not upset the fringe spacing since fringes form parallel to X_1; u_2 and u_3 are not detected unless there is a misalignment of the illuminating beams; and, rigid-body translation along X_1 only causes the fringe pattern to sweep over the specimen but does not introduce spurious fringes into the displacement pattern. Hence, the only rigid-body motion affecting the measurement of the thermal strain is caused by rotation about the X_2 axis.

In Fig. 2, X_1, X_2, X_3 and X_1', X_2', X_3' represent a reference and a transformed coordinate system respectively. Axes X_3 and X_3' coincide; and the primed system may be imagined to be obtained from the unprimed by a counter-clockwise rotation of θ about X_3 or X_3'.

The constraints of the model allow the sensitivity direction, X_1', along which measurements are made to be varied with respect to the reference axis, X_1, by rotating the specimen through the angle defined in Fig. 2. Since the reference axes rotate with the specimen and positive θ is measured from X_1 to X_1', in a counter-clockwise direction; positive θ corresponds to a clockwise rotation of the specimen around X_3, X_3'.

Thermal strains ϕ_A, ϕ_H and ϕ_C are determined when direct strain measurements taken from the displacement patterns corresponding to $\theta = 0$ deg, 45 deg and 90 deg are divided by ΔT. These values are sufficient to define the eigenvalues of the thermal-strain tensor.

$$\phi_{1,2} = \frac{1}{2}(\phi_A + \phi_C) \pm \frac{1}{2}\sqrt{(\phi_A - \phi_C)^2 + (2\phi_H - \phi_A - \phi_C)^2} \tag{12}$$

with corresponding eigenvectors defined by

$$\tan 2\theta = \frac{2\phi_H - \phi_A - \phi_C}{\phi_A - \phi_C} \tag{13}$$

The solution of eq (13) gives two values for the angle θ, namely θ_1 which refers to the angle between the X_1 axis and the axis corresponding to the maximum principal thermal strain ϕ_1 and, θ_2, which is the angle between the X_1 axis and the axis corresponding to the minimum principal thermal strain, ϕ_2.

Experimental

As shown in Fig. 2, the model was constrained with a screw which passed through the thickness of the specimen into a round cylindrical bar having the same diameter as the screw head. Asbestos was glued to the screw and to the bar where they made contact with the rock in an effort to minimize heat transfer from the rock to its

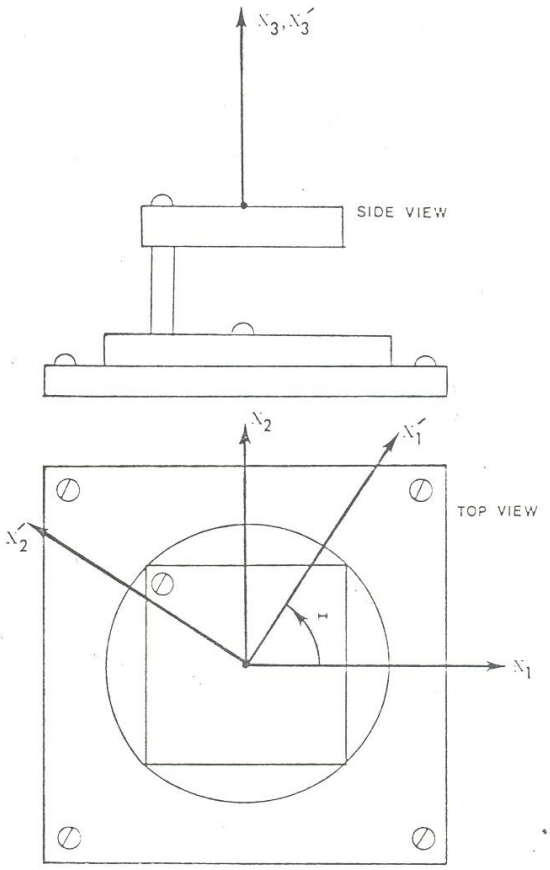

Fig. 2—Model and constraints

constraints. The steel bar was mounted on a circular disk whose center coincided with the center of the model. This allowed the model to be rotated to any desired position for experimental purposes. Rapid, continuous measurements could be made without any other modification of the experimental setup.

In order to initiate a uniform temperature change throughout the model, heating coils were bonded to the four edges of the square specimen parallel to the X_1 axis. A copper sheet was initially applied to each edge of the rock in order to distribute heat evenly on these surfaces. Mica, a paper-thin mineral, was positioned between the copper and the heating coils to provide electrical insulation as well as good thermal conductivity. Finally, a layer of asbestos was applied to ensure heat conduction into the rock. The adhesive used for bonding of the layers to the edge of the specimen was M-Bond 600, a Micro-Measurements product. The four coils bonded to each side of the rock were connected to separate variacs, calibrated to produce a uniform temperature distribution throughout the model.

Temperature was monitored with five Micro-Measurements, type TG, temperature sensors placed on the back side of the specimen as shown in Fig. 3. Prior to the application of the temperature sensors, a thin layer of

Elmers epoxy was used to treat the specimen to eliminate minute voids inherent in the rock surface. Each gage was then bonded to the back surface using M-bond 600. Gage protection and thermal insulation were simultaneously provided by applying M-Coat D, another Micro-Measurements product. The temperature sensors were gages whose resistance varied as a function of surface temperature. Each gage was used in conjunction with an LST network on a quarter-bridge circuit to yield output in microstrain due to temperature change alone.

An effort was made to check the temperature gradient across the thickness of the specimen prior to bonding all of the heating coils to the edges of the model. In this test, the specimen was heated with only one of the four coils. The temperature distribution was measured across the thickness of the specimen on the edge opposite the active coil using thermocouples in conjunction with a meter having digital readout. The temperature gradient across the thickness of the specimen was found to be nearly constant.

A detailed drawing of the experimental setup for the determination of the in-plane displacement appears in Fig. 4. The front-surface mirror positioned normal to the model surface allows two collimated object beams to be constructed from a single source. Experiments can be conducted using a lower-powered laser than would ordinarily be required if the two object beams were produced by a second beam splitter. Figure 5 illustrates the technique in greater detail.

The experimental setup was initially used to measure thermally induced strain for a steel calibration specimen. Results obtained for several values of θ indicated thermally isotropic behavior and verified the sensitivity angle, β, to be 45 deg. All tests were carried out with an argon-ion laser with $\lambda = 2025 \times 10^{-8}$ in. (5145×10^{-5} cm).

The rock specimen was then oriented to measure displacement for $\theta = 0$ deg. The undeformed model state

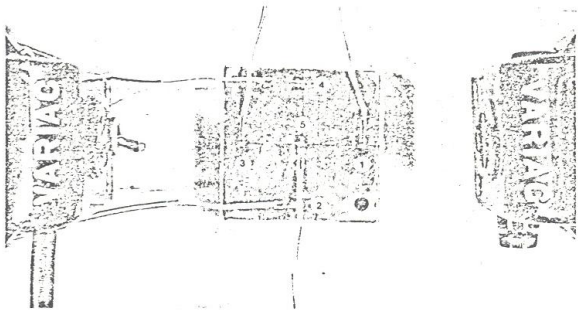

Θ	GAGE 1	GAGE 2	GAGE 3	GAGE 4	GAGE 5
0	10.2	10.1	10.4	10.4	9.0
45	10.2	10.0	10.4	10.4	9.0
90	10.2	10.0	10.0	10.0	8.9

ALL VALUES IN F

Fig. 3—Temperature gages, variacs and values of ΔT

was captured on the photographic plate at room temperature and an initial temperature reading was recorded for each of the five gages shown in Fig. 3. The four variacs

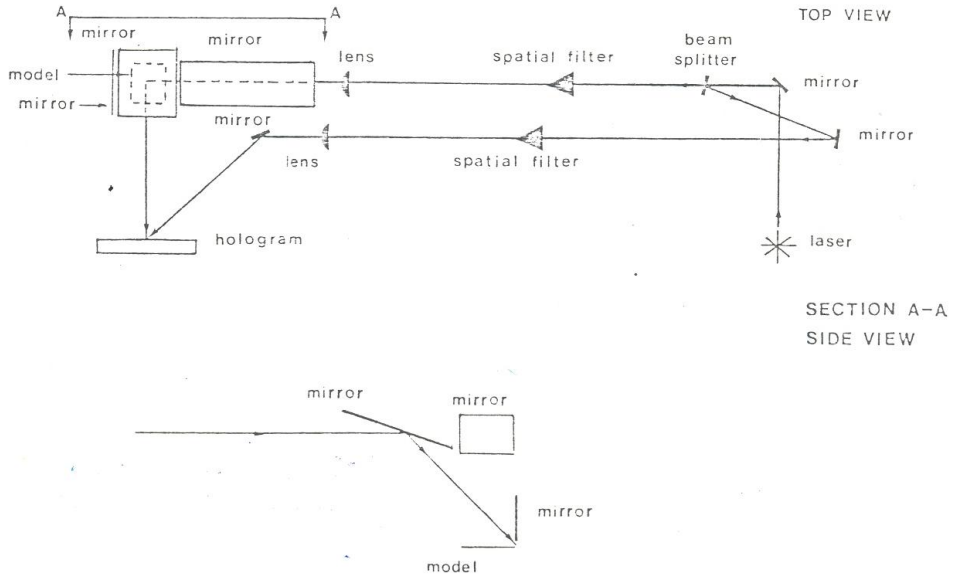

Fig. 4—Experimental setup

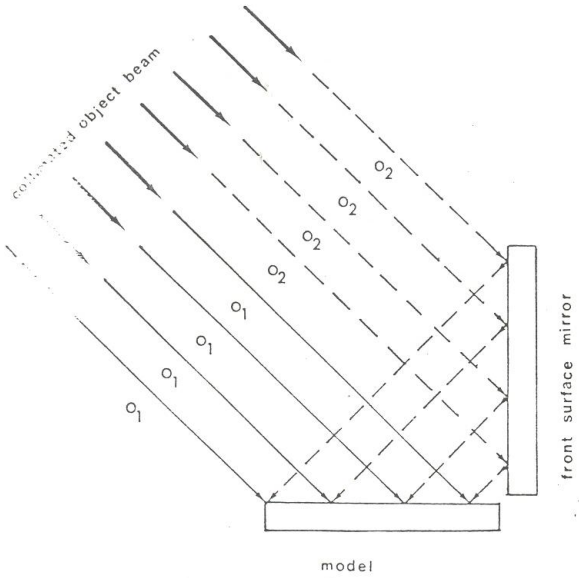

Fig. 5—Illumination of the model

were adjusted to initiate a temperature change to the specimen through the coils bonded to each edge. The photographic plate was rotated to facilitate the formation of a moiré and a second exposure was taken. The final temperature on each gage was recorded and the photographic plate was developed and reconstructed.

The model was rotated and this procedure was repeated for θ equal to 45 deg and 90 deg. Figure 3 documents the temperature changes measured by each of the five temperature gages during each test. Gage numbers are also specified in the figure.

It is extremely important to wait until the model has reached a steady stage before recording the second exposure. A superposition of the second hologram when the model is in an unsteady condition causes extraneous variations in optical path to occur due to temperature gradients and convection currents in the air surrounding the specimen. These additional phase changes are transient over the exposure and are recorded as time-average effects which tend to obscure the deformation pattern.

For a given value of θ, it is evident from Fig. 3 that variacs were adjusted so that the temperature increments measured by gages 1-4 agreed to within three percent; however, gage 5 predicted a temperature change which was consistently lower than the average increment read on gages 1-4 by 14 $\pm$1 percent.

The examination of a typical displacement pattern like that shown in Fig. 6 gives little indication of this temperature difference. Moiré fringes are nearly parallel and equally spaced, indicating that the corresponding strain field is homogeneous over the surface of the model. Although a lower temperature increment is measured by gage 5 due to heat loss through the lateral surfaces, interior points in the central portion of the specimen must experience temperature changes comparable to those measured by gages 1-4 in order to preserve the homogeneous strain field indicated by the experimental patterns.

Strain was determined for the point at the center of the specimen for each value of θ by taking the slope of the plot of displacement vs. distance along the sensitivity direction at the center point of the model. This plot was

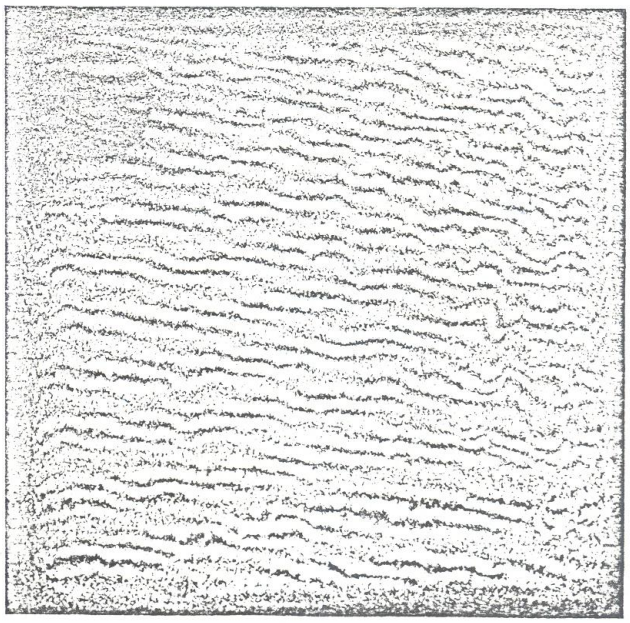

Fig. 6—Typical displacement pattern (θ = 90 deg)

found to be linear for each test, confirming that the strain field was indeed homogeneous. Strains were converted to thermal strain by dividing by an average ΔT calculated from

$$\Delta T = \frac{\Delta T_1 + \Delta T_2 + \Delta T_3 + \Delta T_4 + 2\Delta T_5}{6} \quad (14)$$

where ΔT are the increments obtained from temperature gages 1-5. The experimentally measured thermal strains ϕ_A, ϕ_B and ϕ_C corresponding to $\theta = 0$ deg, 45 deg and 90 deg, respectively, were

$$\phi_A = 2.54 \times 10^{-6} \text{ in./in./°F}$$

$$\phi_B = 2.58 \times 10^{-6} \text{ in./in./°F} \quad (15)$$

$$\phi_C = 6.19 \times 10^{-6} \text{ in./in./°F}$$

When eq (15) is substituted into eqs (12) and (13), principal values and corresponding directions of Φ are given as

$$\phi_1 = \alpha_1 = 6.98 \times 10^{-6} \text{ in./in./°F} \ @ \ \theta_1 = -67.8 \text{ deg}$$

$$\phi_2 = \alpha_2 = 1.81 \times 10^{-6} \text{ in./in./°F} \ @ \ \theta_2 = 22.2 \text{ deg} \quad (16)$$

Additional experiments were carried out with the model oriented in the principal directions and at θ equal to 15 deg. ϕ_1 and ϕ_2 agreed to within 2.0 percent of the values predicted by eq (16). For the intermediate orientation with θ equal to 15 deg, the experimentally determined value for the thermal strain was

$$\phi_{15} = 5.13 \times 10^{-6} \text{ in./in./°F} \quad (17)$$

When the measured values documented in eq (15) are used in conjunction with eq (2), a predicted value of thermal strain,

$$\phi_{15} = 5.05 \times 10^{-6} \text{ in./in./°F} \quad (18)$$

results. Values in eqs (17) and (18) agree to within 1.6-percent error.

The directions documented in eq (16) determine the orientation of layers in the specimen, assuming that layers are oriented perpendicular and parallel to the principal-strain directions in the X_1X_2 plane. Results indicate that Bedford limestone expands through α_1 perpendicular to its layers and through α_2 parallel to them. Furthermore, under the assumption that the thermal coefficient of expansion is independent of direction parallel to stratification,

$$\alpha_3 = \alpha_2 = 1.81 \times 10^{-6} \text{ in./in./°F} \quad (19)$$

The values obtained for α_i fall within the range of the thermal coefficients of expansion documented during other investigations involving Bedford limestone.[11-13] Values of α range from 7.9×10^{-6} in./in./°F to 1.6×10^{-6} in./in./°F for experiments conducted at or about room temperature. These values compare well with the maximum and minimum thermal coefficients of expansion measured holographically. The maximum value determined in this study is 11 percent less than the maximum value previously documented, while the minimum value determined in this study is 11 percent greater than the minimum value previously documented.

It should be pointed out that measurements made during these other investigations require specimens to be subjected to substantial temperature changes, on the order of a few hundred degrees Fahrenheit, over which thermal properties are assumed linear. The high sensitivity of holography, however, allows thermal behavior of rock specimens to be analyzed when they are subjected to small temperature changes, on the order of a few degrees Fahrenheit. This suggests that small, successive temperature increments could be initiated to a rock specimen in order to investigate the linearity of its thermal properties.

Conclusions

This study has demonstrated that holography is a useful tool for the analysis of homogeneous strains caused by uniform temperature changes. Although experiments were carried out for a single type of sedimentary rock, the methods developed are universally applicable to all types of rock and lay a firm foundation to support other holographic investigations in experimental rock mechanics.

The optical-rosette concept is also an important outgrowth of this study. Although this method of attack could be used to analyze mechanical deformation, it is particularly well suited to study thermally induced deformation, especially in materials whose thermal coefficients of expansion are positive.

Acknowledgment

This investigation was made possible through a grant from the Graduate School at the University of Wisconsin-Milwaukee and National Science Foundation Grant No. SER 77-06858. Special thanks is extended to H. Pincus, professor of geological sciences, for his helpful suggestions and comments made throughout the study.

References

1. Lee, C.F. and Klyn, T.W., "Stability of Heated Caverns in a High Horizontal Stress Field," Proceedings, First International Symposium on Storage in Excavated Caverns, Stockholm, 3 (1977).

2. Bjurstrom, S., "Transport and Storage of Hot Water in Unlined Rock Openings," Proceedings, First International Symposium on Storage in Excavated Caverns, Stockholm, 3 (1977).

3. Milne, L.A., Giramonti, A.J., and Lessard, R.D., "Compressed Air Storage in Hard Rock for Use in Power Applications," Proceedings, First International Symposium on Storage in Excavated Caverns, Stockholm, 3 (1977).

4. Soderberg, L., "Practical Procedure for Preinvestigations Concerning Unlined Rock Storage Caverns for Petroleum Products," Proceedings First International Symposium on Storage in Excavated Caverns, Stockholm, 3 (1977).

5. Muse, G.E., Continuum Mechanics, McGraw-Hill (1970).

6. Sciammarella, C.A. and Gilbert, J.A., "A Holographic-moiré Technique to Obtain Separate Patterns for Components of Displacement," EXPERIMENTAL MECHANICS, 16 (6), 215-220 (1976).

7. Gilbert, J.A., Sciammarella, C.A. and Chawla, S.K., "Extension to Three Dimensions of a Holographic-moiré Technique to Separate Patterns Corresponding to Components of Displacement," EXPERIMENTAL MECHANICS, 18 (9), 321-327 (1978).

8. Gilbert, J.A., "Differentiation of Holographic-moiré Patterns," EXPERIMENTAL MECHANICS, 18 (11), 436-440 (1978).

9. Sciammarella, C.A. and Chawla, S.K., "A Lens Holographic-moiré Technique to Obtain Components of Displacement and Derivatives," EXPERIMENTAL MECHANICS, 18 (10), 373-381 (1978).

10. Denby, D. and Leendertz, J.A., "Plane-Surface Examination by Speckle-Pattern Interferometry Using Electronic Processing," J. of Strain Analysis, 9 (1) (1974).

11. Desai, P.D., Navarro, R.A., Hasan, S.E., Ho, C.Y., DeWitt, D.P. and West, T.R., "Thermophysical Properties of Selected Rock," Center for Information and Numerical Data Analysis and Synthesis, TPRC Report 23 (1974).

12. Souder, W.H. and Hubert, P., "Thermal Expansion of Building Materials," United States National Bureau of Standards Science Papers, 15 (1919).

13. Harvey, R.D., "Thermal Expansion of Certain Illinois Limestone and Dolomites," Illinois State Geological Survey Circulation, No. 415 (1967).